



Gen. Math. Notes, Vol. 27, No. 1, March 2015, pp. 55-68

ISSN 2219-7184; Copyright © ICSRS Publication, 2015

www.i-csrs.org

Available free online at <http://www.geman.in>

Numerical Study for Heat Transfer in Symmetric Porous Channel with Expanding or Contracting Walls and Slip Boundary Condition

K. Raslan¹ and Zain F. Abu Shaer²

^{1,2}Department of Mathematics, Faculty of Science
Al-Azhar University, Egypt

¹E-mail: kamal_raslan@yahoo.com

²E-mail: zainfathi@hotmail.com

(Received: 22-11-14 / Accepted: 1-2-15)

Abstract

The homotopy analysis method (HAM) is implemented to obtain the approximate solutions of the nonlinear evolution equations in mathematical physics. The results obtained by this method have a good agreement with one obtained. It illustrates the validity and the great potential of the homotopy analysis method in solving partial differential equations.

Keywords: *HAM, Porous channel; Expanding and contracting walls Slip boundary condition; Heat transfer.*

1 Introduction

The flow in channels and in circular pipes with permeable walls has received considerable attention in the past few years. The earliest work of steady flow

across permeable and stationary walls can be traced back to Berman [1], who showed that the governing equations can be reduced to single fourth-order nonlinear ordinary differential equation which includes permeation Reynolds number \mathcal{R}_e , and associated solution can be obtained. Laminar flow studies in porous pipes or channels with expanding or contracting walls have received considerable attention due to their applications in biophysical flows. These include the model of pulsating diaphragms, filtration, blood flow and artificial dialysis, binary gas diffusion, the model of air and blood circulation in the respiratory system. In order to simulate the peristaltic motion by successive wall contractions and expansions. Uchida and Aoki [15] first examined the viscous flow inside an impermeable tube with contracting cross sections. Ohki [20] investigated the unsteady flow in a porous semi-infinite tube, whose elastic wall had a varied length and a stable cross section. To simulate the laminar flow in cylindrical solid rocket motors, Goto and Uchida [4] analyzed the laminar incompressible flow in a semi-infinite porous pipe, whose radius varied with time. Bujurke et al. [3] obtained a series solution to the unsteady flow in a contracting or expanding pipe. Majdalani et al. [6] obtained an exact similarity solution to the viscous flow with small wall contractions or expansions and weakly permeability. Dauenhauer and Majdalani [5] obtained a numerical solution and Majdalani and Zhou [7] got both numerical and asymptotical solutions for moderate to large Reynolds numbers. Srinivasacharya [14] obtained a numerical solution to the flow and heat transfer of couple stress fluid in a porous channel with expanding and contracting walls. Si et al. [13] obtained analytic solution to the micro-polar-fluid flow through a semi-porous channel with an expanding or contracting wall. Dinarvand [10] studied viscous flow through slowly expanding or contracting porous walls with low seepage Reynolds number: a model for transport of biological fluids through vessels.

No-slip condition was no longer valid at the permeable surface. Some of both experimental and theoretical studies stated that slip could not be ruled out as a significant element in the understanding of certain flow peculiarities [17]. Beavers, Joseph [2] reported mass efflux experiments and proved the existence of a non-zero tangential (slip) velocity on the surface of a permeable boundary. Using a statistical approach, Saffman [12] derived a form for the slip velocity. Isenberg [8] posited slip for all practical purposes in his study of blood flow in capillary tubes. However, very little reports were found in literature for micropolar fluids with expanding or contracting walls and slip boundary condition. Bennett [11] reported that microscopic examination of blood flowing past a glass wall shown slipping (skidding) of red cells in contact with the wall. Chellam et al. [9] investigated the effect on fluid flow and mass transfer with slip at a uniformly porous boundary.

Recently, Zhang and Jia [18, 19] discussed the Navier-Stokes equations with first-order and second-order accurate slip boundary conditions for describing the two-dimensional gaseous steady laminar flow between two plates. Ramos [16] obtained an asymptotic analytical solution of channel flows of incompressible

fluids with a slip length that depended on the pressure and/or the axial pressure gradient.

The series solutions are presented by HAM developed by Liao [21-23], which has been successfully applied to several nonlinear problems by Hayat, Noor and Hashim [25, 26]. In this paper, the effects of different parameters, especially expansion ratio and slip coefficient, on velocity and temperature are studied and shown graphically.

The main goal of this paper is to find the numerical solutions for the heat transfer in symmetric porous channel with expanding or contracting walls and slip boundary conditions. This second section will give statement of the problem and governing equations. In section 3, computations by Homotopy analysis method. Finally, the graphs for velocity components and heat transfer presented for different values of the fluid parameters are plotted and discussed.

2 Statement of the Problem and Governing Equations

Consider the unsteady two-dimensional motion of an incompressible fluid with heat transfer in a porous semi-infinite channel with expanding or contracting walls with slip boundary condition. The distance $2a(t)$ between the porous walls is much smaller than the width and length of the channel. One end of the channel is closed by a complicated solid membrane. Both walls have equal permeability V_w and expand or contract uniformly at a time-dependent rate $\dot{a}(t)$. As shown in Fig. 1, a coordinate system may be chosen with the origin at the center of channel. Take \hat{x} and \hat{y} to be co-ordinate axes parallel and perpendicular to the channel walls and assume \hat{u} and \hat{v} to be the velocity components in the \hat{x} and \hat{y} directions respectively and $\hat{\theta}$ is the temperature. Under these assumptions, the governing equations are expanded as follows [27].

$$\left\{ \begin{array}{l} \frac{\partial \hat{u}}{\partial \hat{x}} + \frac{\partial \hat{v}}{\partial \hat{y}} = 0 \\ \rho \left(\frac{\partial \hat{u}}{\partial t} + \hat{u} \frac{\partial \hat{u}}{\partial \hat{x}} + \hat{v} \frac{\partial \hat{u}}{\partial \hat{y}} \right) = -\frac{\partial \hat{p}}{\partial \hat{x}} + \mu \nabla^2 \hat{u} \\ \rho \left(\frac{\partial \hat{v}}{\partial t} + \hat{u} \frac{\partial \hat{v}}{\partial \hat{x}} + \hat{v} \frac{\partial \hat{v}}{\partial \hat{y}} \right) = -\frac{\partial \hat{p}}{\partial \hat{y}} + \mu \nabla^2 \hat{v} \\ \rho c_p \left(\frac{\partial \hat{\theta}}{\partial t} + \hat{u} \frac{\partial \hat{\theta}}{\partial \hat{x}} + \hat{v} \frac{\partial \hat{\theta}}{\partial \hat{y}} \right) = \mu \left[4 \left(\frac{\partial \hat{u}}{\partial \hat{x}} \right)^2 + \left(\frac{\partial \hat{u}}{\partial \hat{y}} + \frac{\partial \hat{v}}{\partial \hat{x}} \right)^2 \right] + K \nabla^2 \hat{\theta}, \end{array} \right. \quad (1)$$

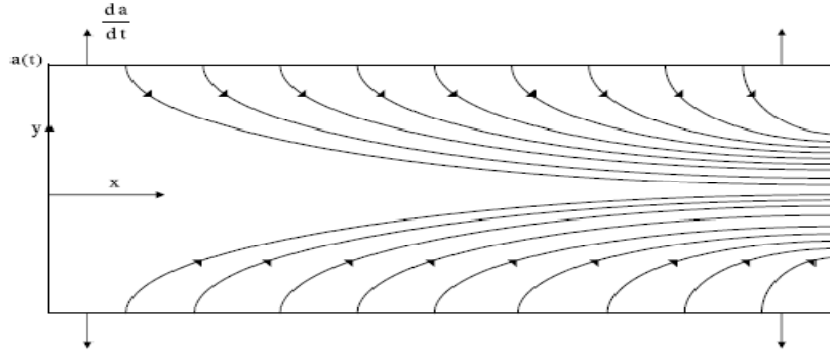


Figure1: Coordinate system and bulk fluid motion

A general infinitesimal group of transformations under which given partial differential equations are invariant [27], the equations (1) are a set of linear differential equations. Ref [27] completed transforms as

$$u = \frac{\partial \psi}{\partial y}, v = -\frac{\partial \psi}{\partial x}, \quad (2)$$

And the stream function takes the form, [24, 27]

$$\psi = x G(y), u = x \frac{dG}{dy}, v = -G, \quad (3)$$

These transforms change the second equation in (1) to,

$$\frac{d^4 G}{dy^4} + \alpha \left(y \frac{d^3 G}{dy^3} + 2 \frac{d^2 G}{dy^2} \right) + \mathcal{R}_e \left(G \frac{d^3 G}{dy^3} - \frac{dG}{dy} \frac{d^2 G}{dy^2} \right) = 0, \quad (4)$$

He Suggest that the form of temperature take as

$$\theta = \theta(x, y) = \zeta(y) + x^2 \chi(y), \quad (5)$$

During the assumption of the third and fourth equation in (1) become

$$\frac{d^2 \chi}{dy^2} + P_r \left[(\alpha y + \mathcal{R}_e G) \frac{d\chi}{dy} + E_c \left(\frac{d^2 G}{dy^2} \right)^2 - 2\mathcal{R}_e \chi \frac{dG}{dy} \right] = 0, \quad (6)$$

$$\frac{d^2 \zeta}{dy^2} + P_r \left[(\alpha y + \mathcal{R}_e G) \frac{d\zeta}{dy} + 4E_c \left(\frac{dG}{dy} \right)^2 \right] + 2\chi = 0,$$

With the boundary conditions

$$\frac{dG(1)}{dy} = -\phi \frac{d^2 G(1)}{dy^2}, \quad G(1) = 1, \quad \zeta(1) = 1, \quad \chi(1) = 0,$$

$$\frac{d^2 G(0)}{dy^2} = 0, \quad G(0) = 0, \quad \zeta(0) = \theta_2, \quad \chi(0) = 0, \quad (7)$$

Where $\mathcal{R}_e = \frac{aV_w}{\nu}$ is permeation Reynolds number, $P_r = \frac{\mu c_p}{K}$ is Prandtl number and $E_c = \frac{aV_w^2}{c_p \theta_0}$ is Eckart number. The wall permeance or injection coefficient A is defined as $A = \frac{\mathcal{R}_e}{a}$, it is a measure of wall permeability. It will be started to solve the nonlinear equations (4) and (6) with the boundary conditions.

3 Computations by Homotopy Analysis Method [21-23]

From the rule of solution expression and the boundary conditions (7) it is straightforward to choose the following initial guesses.

$$G_0(y) = \frac{y(6\varphi+3-y^2)}{2(1+3\varphi)}, \quad \chi_0(y) = \frac{y(6\varphi+3-y^2)}{2(1+3\varphi)}, \quad \text{and} \quad \zeta_0(y) = \theta_2 + (1 + \theta_2)y, \quad (8)$$

The linear operators are selected as

$$\mathcal{L}_1 = \frac{d^4 G}{dy^4}, \quad \mathcal{L}_2 = \frac{d^2 \chi}{dy^2}, \quad \text{and} \quad \mathcal{L}_3 = \frac{d^2 \zeta}{dy^2}, \quad (9)$$

These operators satisfy the following properties:

$$\begin{aligned} \mathcal{L}_1(C_1 y^3 + C_2 y^2 + C_3 y + C_4) &= 0, \quad \mathcal{L}_2(C_5 y + C_6) = 0, \quad \text{and} \\ \mathcal{L}_3(C_7 y + C_8) &= 0, \end{aligned} \quad (10)$$

Where C_i ($i = 1 - 8$) are the constants.

Upon making use of above definitions, we construct the zero-order deformation problems

$$(1-p)\mathcal{L}_1(\hat{G} - G_0) = p \hbar \mathfrak{N}_1(\hat{G}, \hat{\chi}), \quad (11)$$

$$\hat{G}'(1,p) = -\phi \hat{G}''(1,p), \quad \hat{G}(1,p) = 1, \quad \hat{G}''(0,p) = 0, \quad \hat{G}(0,p) = 1, \quad (12)$$

$$(1-p)\mathcal{L}_2(\hat{\chi} - \chi_0) = p \hbar \mathfrak{N}_2(\hat{G}, \hat{\chi}), \quad (13)$$

$$\hat{\chi}(1,p) = 0, \quad \hat{\chi}(0,p) = 1, \quad (14)$$

$$(1-p)\mathcal{L}_3(\hat{\zeta} - \zeta_0) = p \hbar \mathfrak{N}_3(\hat{G}, \hat{\chi}, \hat{\zeta}), \quad (15)$$

$$\hat{\zeta}(1,p) = 1, \quad \hat{\zeta}(0,p) = \theta_2, \quad (16)$$

$$\mathfrak{K}_1(\hat{G}, \hat{\chi}) = \frac{\partial^4 \hat{G}}{\partial y^4} + \alpha \left(y \frac{\partial^3 \hat{G}(y,p)}{\partial y^3} + 2 \frac{\partial^2 \hat{G}(y,p)}{\partial y^2} \right) + \mathcal{R}_e \left(\frac{\partial^3 \hat{G}(y,p)}{\partial y^3} \hat{G}(y,p) - \frac{\partial \hat{G}(y,p)}{\partial y} \frac{\partial^2 \hat{G}(y,p)}{\partial y^2} \right) \quad (17)$$

$$\mathfrak{K}_2(\hat{G}, \hat{\chi}) = \frac{\partial^2 \hat{\chi}(y,p)}{\partial y^2} + P_r \left((\alpha y + \mathcal{R}_e \hat{G}(y,p)) \frac{\partial \hat{\chi}(y,p)}{\partial y} + E_c \left(\frac{\partial^2 \hat{G}(y,p)}{\partial y^2} \right)^2 - 2 \mathcal{R}_e \hat{\chi}(y,p) \frac{\partial \hat{G}(y,p)}{\partial y} \right) \quad (18)$$

$$\mathfrak{K}_3(\hat{G}, \hat{\chi}) = \frac{\partial^2 \hat{\zeta}(y,p)}{\partial y^2} + P_r \left((\alpha y + \mathcal{R}_e \hat{G}(y,p)) \frac{\partial \hat{\zeta}(y,p)}{\partial y} + 4 E_c \left(\frac{\partial \hat{G}(y,p)}{\partial y} \right)^2 \right) + 2 \hat{\chi}(y,p), \quad (19)$$

If $p \in [0, 1]$ is an embedding parameter and \hbar are the nonzero auxiliary parameters then the zeroth-order deformation problems can be constructed as [15] respectively. Using Taylor's theorem, we can write

$$\hat{G}(y, p) = \hat{G}_0(y) + \sum_{m=1}^{\infty} \hat{G}_m(y) p^m, \quad \hat{G}_m(y) = \frac{1}{m!} \frac{\partial^m \hat{G}(y,p)}{\partial p^m}, \quad (20)$$

$$\hat{\chi}(y, p) = \hat{\chi}_0(y) + \sum_{m=1}^{\infty} \hat{\chi}_m(y) p^m, \quad \hat{\chi}_m(y) = \frac{1}{m!} \frac{\partial^m \hat{\chi}(y,p)}{\partial p^m}, \quad (21)$$

$$\hat{\zeta}(y, p) = \hat{\zeta}_0(y) + \sum_{m=1}^{\infty} \hat{\zeta}_m(y) p^m, \quad \hat{\zeta}_m(y) = \frac{1}{m!} \frac{\partial^m \hat{\zeta}(y,p)}{\partial p^m}, \quad (22)$$

The convergence of the two series is strongly dependent upon \hbar . Assume that \hbar is chosen so that the series (20-22) are convergent at $p = 1$. From Equations (20-22), we have

$$G(y, p) = G_0(y) + \sum_{m=1}^{\infty} G_m(y), \quad (23)$$

$$\chi(y, p) = \chi_0(y) + \sum_{m=1}^{\infty} \chi_m(y), \quad (24)$$

$$\zeta(y, p) = \zeta_0(y) + \sum_{m=1}^{\infty} \zeta_m(y), \quad (25)$$

Differentiating Equations (14) and (16) m times with respect to p , then setting $p = 0$ and finally dividing them by $m!$, we obtain the following m^{th} -order deformation problems.

$$\mathcal{L}_1(G_m(y) - \mathcal{Z}_m G_{m-1}(y)) = \hbar \mathfrak{R}_m^G(y), \quad (26)$$

$$G'_m(1) = -\phi G''_m(1), \quad G_m(1) = 0, \quad G''_m(0) = 0, \quad \text{and} \quad G_m(0) = 0, \quad (27)$$

$$\mathfrak{R}_m^G(y) = G_{m-1}^{(4)} + \alpha(y G_{m-1}''' + 2 G_{m-1}'') + \sum_{k=0}^{m-1} \mathcal{R}_e(G_{m-k-1} G_k'' - G'_{m-k-1} G_k''), \quad (28)$$

$$\mathcal{L}_2(\chi_m(y) - \mathcal{Z}_m \chi_{m-1}(y)) = \hbar \mathfrak{R}_m^\chi(y), \quad (29)$$

$$\chi_m(0) = 0, \chi_m(1) = 0, \tag{30}$$

$$\mathfrak{R}_m^\chi(y) = \chi_{m-1}'' + Pr((\alpha y)\chi_{m-k-1}' + \mathcal{R}_e \sum_{k=0}^{m-1} (G_{m-k-1}\chi_m' - 2\chi_{m-k-1}G_k') + E_c G_{m-k-1}'' G_k''), \tag{31}$$

$$\mathcal{L}_3(\zeta_m(y) - \mathcal{Z}_m \zeta_{m-1}(y)) = \hbar \mathfrak{R}_m^\zeta(y), \tag{32}$$

$$\zeta_m(0) = \theta_2, \zeta_m(1) = 1, \tag{33}$$

$$\mathfrak{R}_m^\zeta(y) = \zeta_{m-1}'' + Pr[(\alpha y)\zeta_{m-k-1}' + \mathcal{R}_e \sum_{k=0}^{m-1} (f_{m-k-1}\zeta_m' + 4E_c G_{m-k-1}' G_k')] + 2\chi_{m-1}'', \tag{34}$$

Where

$$\mathcal{Z}_m = \begin{cases} 0, & m \leq 1, \\ 1, & m > 1. \end{cases} \tag{35}$$

The general solutions of Equations (26), (29) and (32) are

$$G_m(y) = G_m^*(y) + C_1 + C_2 y + C_3 y^2 + C_4 y^3, \tag{36}$$

$$\chi_m(y) = \chi_m^*(y) + C_5 + C_6 y, \tag{37}$$

$$\zeta_m(y) = \zeta_m^*(y) + C_7 + C_8 y, \tag{38}$$

in which $G_m^*(y), \chi_m^*(y)$ and $\zeta_m^*(y)$ denote the special solutions of Equations (26), (29) and (32) and the integral constants C_i ($i = 1 - 8$) are determined by employing the boundary conditions (27), (30) and (33). In this way, it is easy to solve the linear nonhomogeneous. Equations (26), (29) and (32) by using Mathematica one after the other in the order $m = 1, 2, 3, \dots$

$$G(y) = \left(\frac{y}{7761600(1+3\phi)^5} (-3880800(-3 + y^2 - 6\phi)(1 + 3\phi)^4 - 55440(-1 + y^2)(1 + 3\phi)^2(\mathcal{R}_e(-2 + y^2 + y^4 + 3(-6 + y^2 + y^4)\phi) + 21\alpha(1 + 3\phi)(-1 - 7\phi + y^2(1 + 3\phi)))\hbar + (-1 + y^2)(-2772\alpha(1 + 3\phi)^2(25y^4\alpha(1 + 3\phi)^2 - 210(1 + 3\phi)(1 + 7\phi) - 2y^2(1 + 3\phi)(-105 + 19\alpha + 15(-21 + 8\alpha)\phi) + \alpha(13 + 3\phi(52 + 285\phi))) + 6\mathcal{R}_e^2(703 + 14y^8(1 + 3\phi)^2 - 7y^6(1 + 3\phi)^2(53 + 110\phi) - y^2(1 + 3\phi)(173 + 7\phi(71 + 330\phi)) - y^4(1 + 3\phi)(173 + 7\phi(71 + 330\phi)) + \phi(11248 + 21\phi(2063 + 3630\phi))) - 77R(1 + 3\phi)(65y^6\alpha(1 + 3\phi)^2 + y^2(1 + 3\phi)(360(1 + 3\phi) + \alpha(227 + 681\phi + 3240\phi^2)) + y^4(1 + 3\phi)(360(1 + 3\phi) + \alpha(389 + 15\phi(121 + 216\phi))) - 3(240(1 + 3\phi)(1 + 9\phi) + \alpha(227 + \phi(3178 + 3\phi(3793 + 6480\phi))))))\hbar^2 \right), \tag{39}$$

If we take $\phi \rightarrow 0$, we get

$$G(y) = \left(\frac{-y^3}{2} + \frac{3y}{2} + 3\alpha \left(\frac{y^5}{40} - \frac{y^3}{20} + \frac{y}{40} \right) + \mathcal{R}_e \left(\frac{y^7}{280} - \frac{3y^3}{280} + \frac{y}{140} + \alpha \left(-\frac{13\mathcal{R}_e y^9 \alpha}{20160} - \frac{9y^7}{2800} + \frac{9y^5}{5600} + \frac{227y^3}{25200} - \frac{227y}{33600} \right) \right) + \mathcal{R}_e^2 \left(\frac{y^{11}}{92400} - \frac{R^2 y^9}{3360} + \frac{3y^7}{19600} + \frac{73y^3}{107800} - \frac{703y}{1293600} \right) + \alpha^2 \left(\frac{-y^7}{112} + \frac{9y^5}{400} - \frac{51y^3}{2800} + \frac{13y}{2800} \right), \quad (40)$$

4 Numerical Results and Discussion

Our computations show that the series solutions converge in the whole region of y when $\hbar_f = \hbar_\theta = -1$. This section deals with the graphics and the interpretation of the dimensionless wall dilation rate α and the slip coefficient ϕ , on the x and y components of the fluid velocity and heat transfer distributions. Table (1), figures 2(a) and 2(b) present the comparison of self-axial velocity u/x profiles between the HAM solutions and Ref. [24] analytical results for $\alpha = \pm 0.5$, $\phi = 0$.

Figures (3–5) show the effect of slip coefficient on the velocity components and the temperature distributions. We can observe that the slip coefficient ϕ has obvious influence on the velocity and the temperature. Fig.2 shows that the axial velocity is a decreasing function of ϕ near to the center. However, it is an increasing function of ϕ near to the walls. However, with the increase in ϕ , the influence of ϕ on the velocity and the temperature becomes smaller. We can also find that the radial velocity is a decreasing function of ϕ in fig. 3. Fig.4 show that the effect of the slip coefficient ϕ on temperature θ , it is obvious that as ϕ increasing the temperature θ decreasing. The influence of the wall expansion ratio α on velocity component u/x is given in Figures (6–11) for fixed ϕ in case of injection $\mathcal{R}_e = 1$ and suction $\mathcal{R}_e = -1$. With the expansion of the wall, the axial velocity increases. The maximum of streamwise velocity lies at the center of the channel whether α is positive and the lower near the wall; however, whether α is negative (contracting wall), increasing contraction ratio leads to lower axial velocity near the center, and the higher near the wall. The axial velocity distribution, in all cases, approaches a cosine profile. Figs. (8 and 11) shows that the effect of the wall expansion ratio α on the temperature θ , It is shown that the temperature is increasing function with α for injection and suction. Figs. (12-14) shows that the effect of the Eckert number E_c , Prandtel number P_r and the initial temperature θ_2 on the temperature distribution, we find that the temperature is increasing function with E_c , P_r and θ_2 .

Table1: Comparison between present work solutions and Ref. [24] for self-axial velocity at $\mathcal{R}_e = 5$, for $\phi = 0, \alpha = -0.5$ and $\alpha = 0.5$

Y	$\alpha = -0.5$			$\alpha = 0.5,$		
	Ref[24]	Present	Percentage error (%)	Ref[24]	Present	Percentage error (%)
0.00	1.5151	1.50268	0.0124254	1.556324	1.5439	0.0124254
0.05	1.51134	1.49901	0.0123324	1.551780	1.53945	0.0123324
0.10	1.50005	1.488	0.0120513	1.538164	1.52611	0.0120513
0.15	1.48118	1.4696	0.0115757	1.515522	1.50395	0.0115757
0.20	1.45465	1.44376	0.0108947	1.483935	1.47304	0.0108947
0.25	1.42038	1.41039	0.00999335	1.443517	1.43352	0.00999335
0.30	1.37826	1.36941	0.00885233	1.394421	1.38557	0.00885233
0.35	1.32817	1.32072	0.00744968	1.336839	1.32939	0.00744968
0.40	1.27002	1.26426	0.00576282	1.271006	1.26524	0.00576282
0.45	1.20371	1.19994	0.00377264	1.197207	1.19343	0.00377264
0.50	1.1292	1.12773	0.00146993	1.115778	1.11431	0.00146993
0.55	1.04651	1.04764	0.00113512	1.027110	1.02824	0.00113512
0.60	0.955722	0.959722	0.00399957	0.931656	0.935656	0.00399957
0.65	0.857047	0.864077	0.00702959	0.829933	0.836962	0.00702959
0.70	0.750818	0.760875	0.0100568	0.722523	0.73258	0.0100568
0.75	0.650349	0.650349	0.0128079	0.610078	0.622886	0.0128079
0.80	0.532795	0.532795	0.0148669	0.493322	0.508189	0.0148669
0.85	0.408567	0.408567	0.0156289	0.373046	0.388675	0.0156289
0.90	0.278066	0.278066	0.014244	0.250109	0.264353	0.014244
0.95	0.141729	0.141729	0.00955104	0.125435	0.134986	0.00955104
1.00	-3.470E-18	0.00000	3.470E-18	3.470E-18	0.00000	3.470E-18

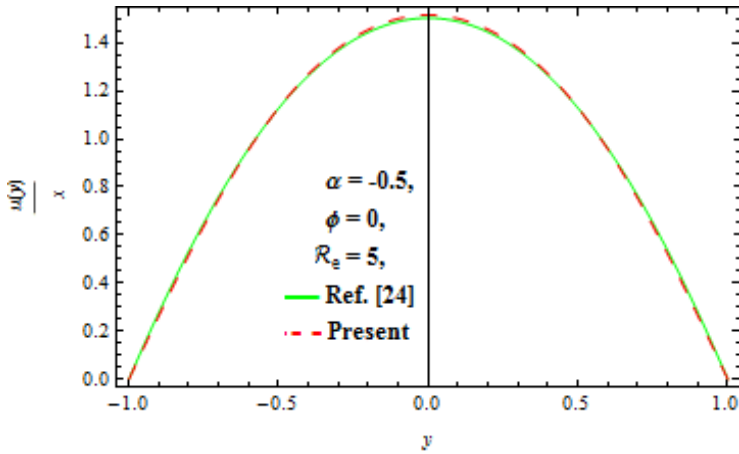


Fig (2a): Comparison between present work solutions and Ref. [24] for self-axial velocity profiles at $\alpha = 0.5$ and $\mathcal{R}_e = 5.0$.

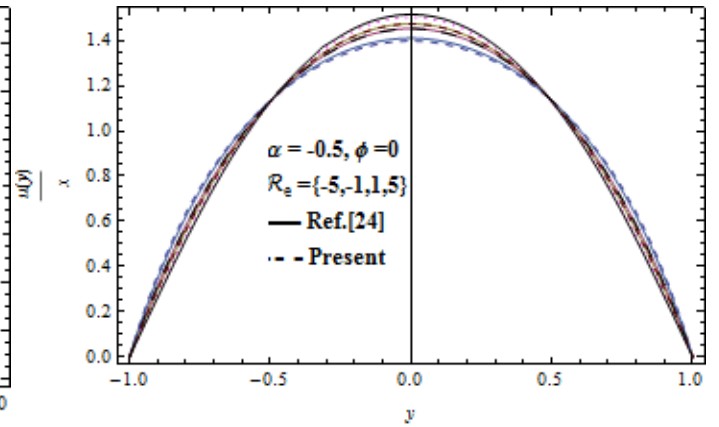


Fig (2b): Self-axial velocity profiles shown over a range of Re at $\alpha = -0.5$, $\phi = 0$

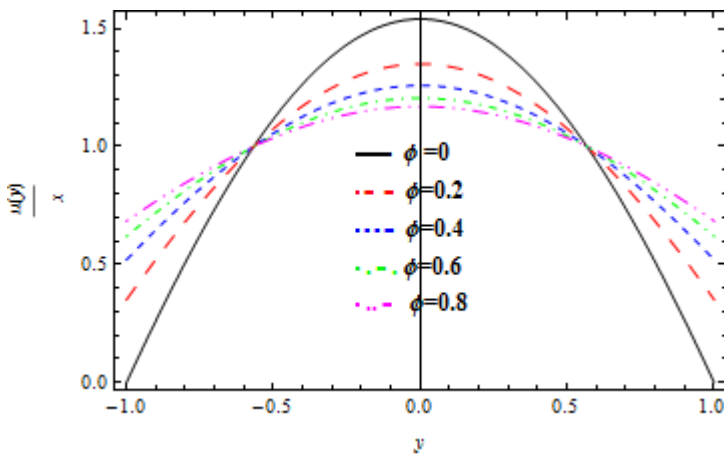


Fig. 3: The effect of the slip coefficient ϕ on the self-axial velocity component with $\mathcal{R}_e=0.5$, $\alpha=0.2$

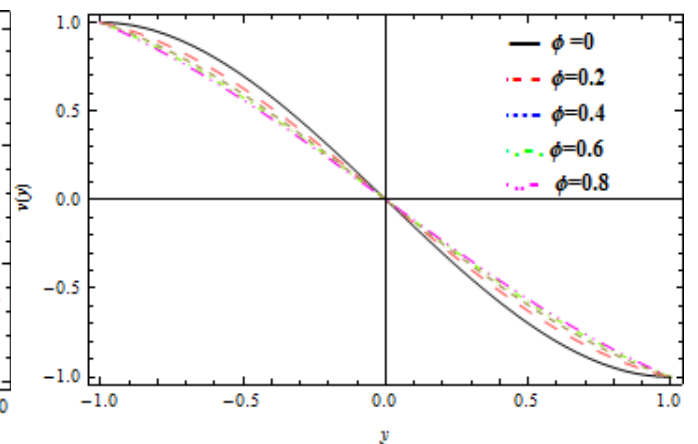


Fig.4: The effect of the slip coefficient ϕ on the radial velocity component with $\mathcal{R}_e=0.5$, $\alpha=0.2$

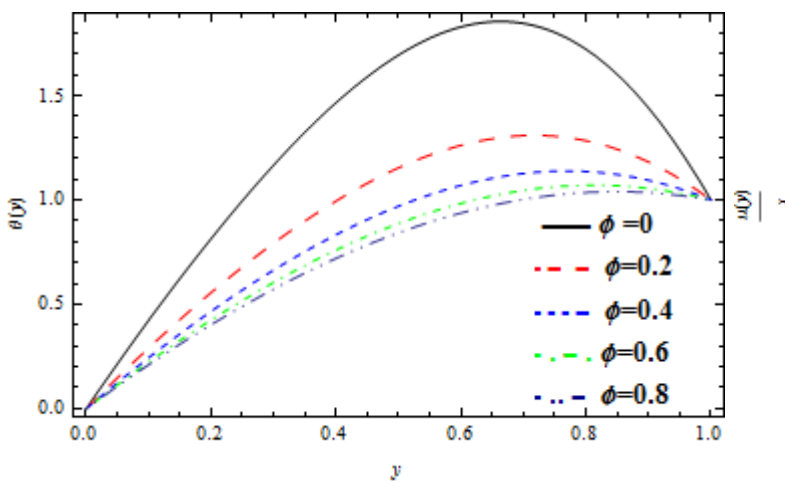


Fig. 5: The effect of the slip coefficient ϕ on temperature distribution with $\mathcal{R}_e = 1$, $\alpha = 0.5$, $\text{Ec} = 0.5$, $\text{Pr} = 0.7$, $\theta_2 = 0$, $x = 3$.

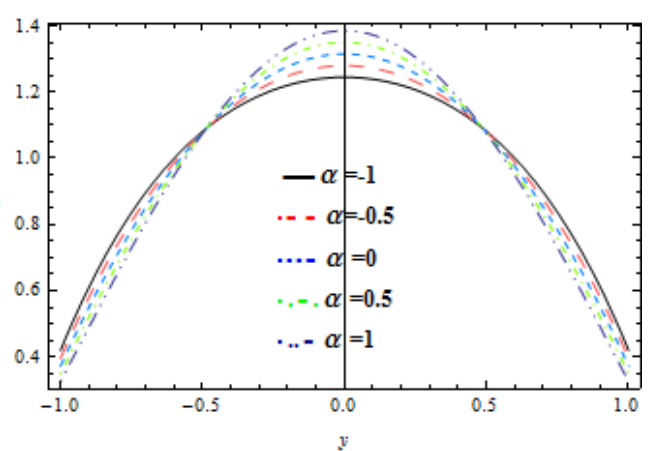


Fig. 6: The effect of the wall expansion ratio α on the self-axial velocity component with $\mathcal{R}_e=1$, $\phi = 0.2$.

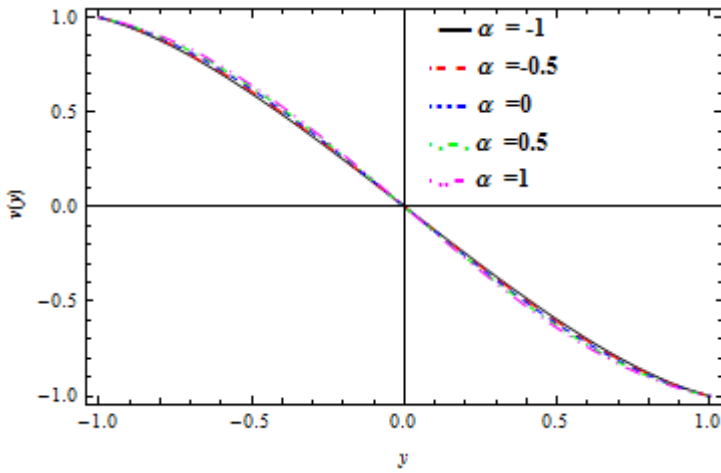


Fig. 7: The effect of the wall expansion ratio α on the radial velocity component with $\mathcal{R}_e = 1$, $\phi=0.2$.

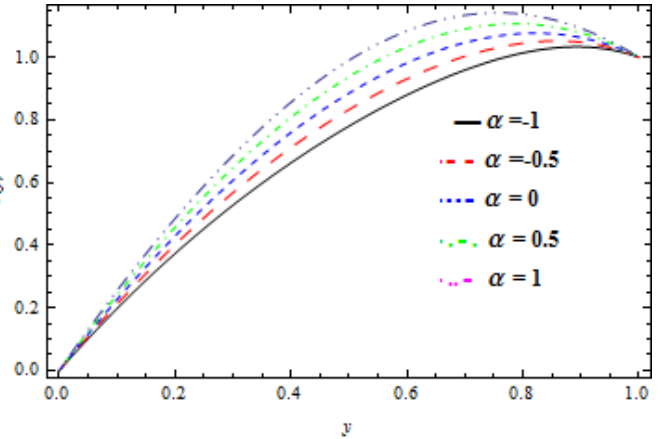


Fig. 8: The effect of the wall expansion ratio α on temperature distribution with $\mathcal{R}_e = 1$, $\phi = 0.2$, $Pr = 0.7$, $Ec=0.5$, $\theta_2 = 0$, $x=3$.

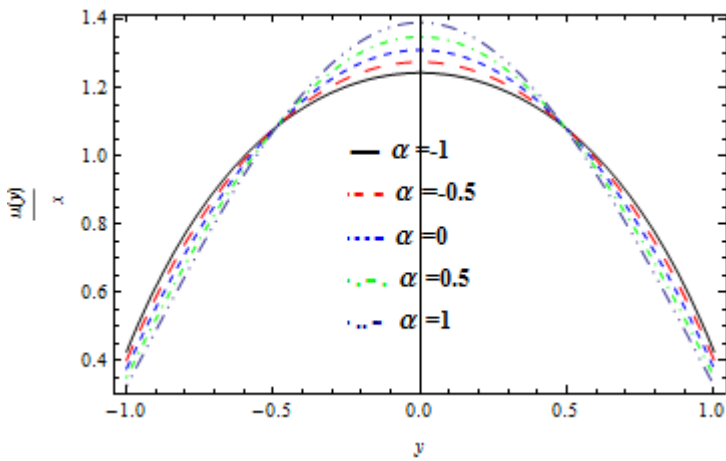


Fig. 9: The effect of the wall expansion ratio α on the self-axial velocity component with $\mathcal{R}_e = -0.5$, $\phi = 0.2$.

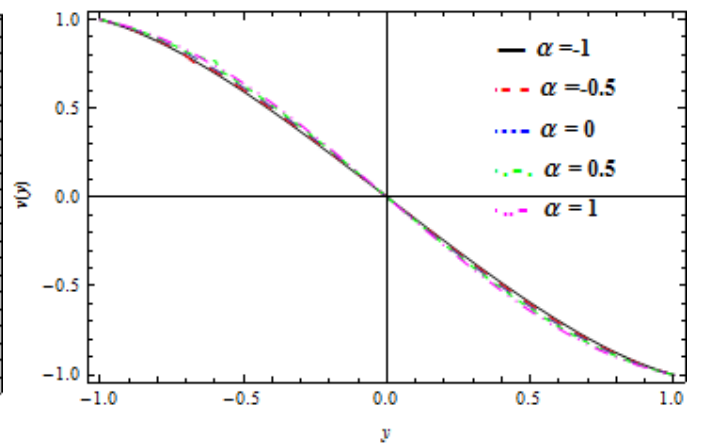


Fig. 10: The effect of the wall expansion ratio α on the radial velocity component with $\mathcal{R}_e = -0.5$, $\phi=0.2$.

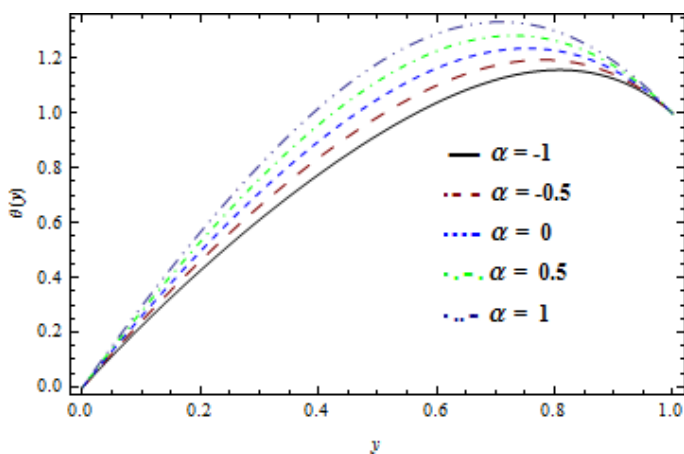


Fig. 11: The effect of the wall expansion ratio α on temperature distribution with $\mathcal{R}_e = -1$, $\phi = 0.2$, $Ec = 0.5$, $Pr = 0.7$, $\theta_2 = 0$, $x=3$

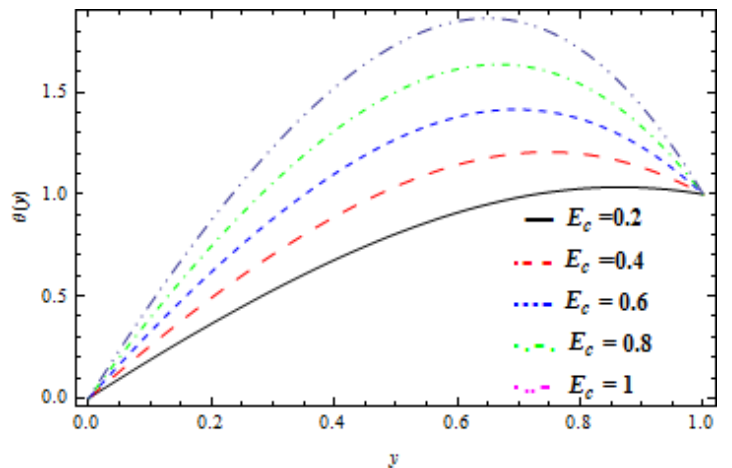


Fig. 12: The effect of the Eckart number E_c on temperature distribution with $\mathcal{R}_e = 1$, $\phi = 0.2$, $\alpha = 0.5$, $Pr = 0.7$, $\theta_2 = 0$, $x=3$.

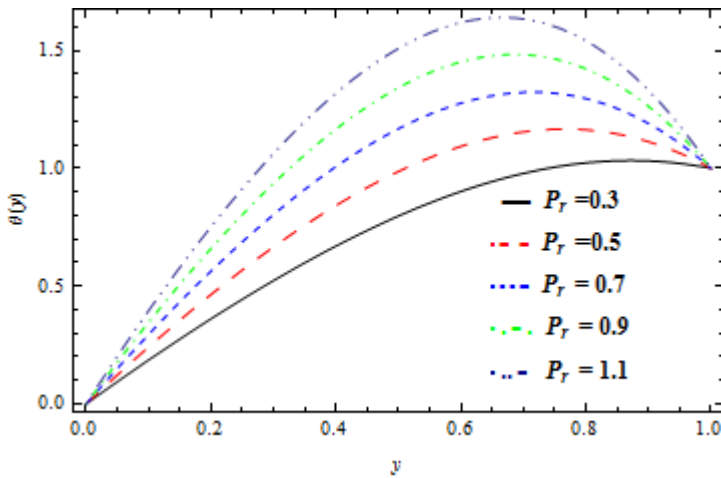


Fig. 13: The effect of Prandtl number Pr on temperature distribution with $\mathcal{R}_e = 0.5$, $\phi = 0.2$, $\alpha = 0.5$, $Ec = 0.5$, $\theta_2 = 0$, $x = 3$.

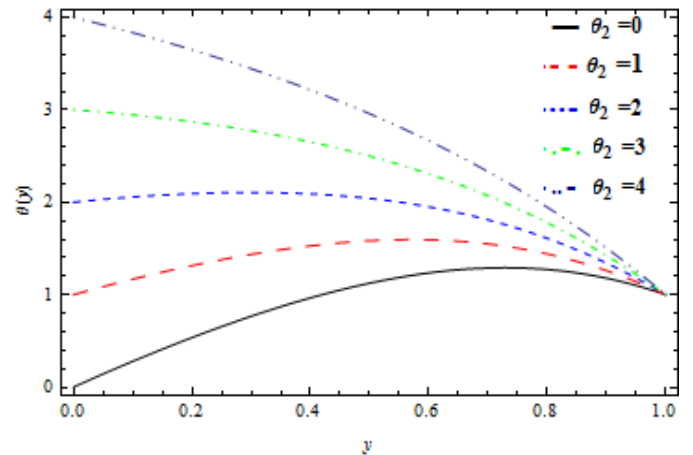


Fig. 14: The effect of θ_2 on temperature distribution with $\mathcal{R}_e = 0.5$, $\phi = 0.2$, $\alpha = 0.5$, $Ec = 0.5$, $Pr = 0.7$, $x = 3$.

5 Conclusion

In this paper, the Homotopy Analysis Method has been applied to study the heat transfer in symmetric porous channel with expanding or contracting walls and slip boundary condition equation. The explicit series solutions our problem are obtained, which are the same as those results given by Lie group analysis method [27] for $\hbar = -1$. In conclusion, HAM provides accurate numerical solution for nonlinear problems in comparison with other methods. It also does not require large computer memory and discretization of the variables x and y . The results show that HAM is powerful mathematical tool for solving nonlinear partial differential equations. Mathematica has been used for computations in this paper.

References

- [1] A.S. Berman, Laminar flow in channels with porous walls, *J. of Appl. Phys.*, 24(1953), 1232-1235.
- [2] G.S. Beavers and D.D. Joseph, Boundary conditions at a naturally permeable wall, *Jour. of Fluid Mech.*, 30(1967), 197-207.
- [3] N.M. Bujurke, N.P. Pai and G. Jayaraman, Computer extended series solution for steady flow in a contracting or expanding pipe, *IMA J. of Appl. Math.*, 60(1998), 151-165.
- [4] M. Goto and S. Uchida, Unsteady flow in a semi-infinite expanding pipe with injection through wall, *J. of the Japan Society for Aer. and Space Sc.*, 33(1990), 14-27.
- [5] C.E. Dauenhauer and J. Majdalani, Exact self-similarity solution of the Navier-Stokes equations for a porous channel with orthogonally moving walls, *Physics. of Fluids*, 15(2003), 1485-1495.

- [6] J. Majdalani, C. Zhou and C.D. Dawson, Two-dimensional viscous flow between slowly expanding or contracting walls with weak permeability, *Jour. of Biomech.*, 35(2002), 1399-403.
- [7] J. Majdalani and C. Zhou, Moderate-to-large injection and suction driven channel flows with expanding or contracting walls, *ZAMM.Z Angew Math Mech.*, 83(2003), 181-196.
- [8] I. Isenberg, A note on the flow of blood in capillary tubes, *Bull. of Math. Biology*, 15(1953), 149-152.
- [9] S. Chellam, M.R. Wiesner and C. Dawson, Slip at a uniformly porous boundary: Effect on fluid flow and mass transfer, *Jour. of Eng. Math.*, 26(1992), 481-492.
- [10] S. Dinarvand, Viscous flow through slowly expanding or contracting porous walls with low seepage Reynolds number: A model for transport of biological fluids through vessels, *Com. Meth. In Biomech. and Biomed. Eng.*, 14(2011), 853-862.
- [11] L. Bennet, Red cell slip at a wall in vitro, *Science (Washington)*, 155(1967), 1554-1556.
- [12] P.G. Saffman, On the boundary condition at the surface of a porous medium, *Studies in Appl. Math.*, 50(1971), 93-101.
- [13] X. Si, L. Zheng, X. Zhang and Y. Chao, Analytic solution to the micropolar-fluid flow through a semi-porous channel with an expanding or contracting wall, *Appl. Math. Mech. Engl. Ed.*, 31(2010), 1073-1080.
- [14] D. Srinivasacharya, N. Srinivasacharyulu and O. Odello, Flow and heat transfer of couple stress fluid in a porous channel with expanding and contracting walls, *Int. Commun. Heat and Mass Transfer*, 36(2009), 180-185.
- [15] S. Uchida and H. Aoki, Unsteady flows in a semi-infinite contracting or expanding pipe, *J Fluid Mech.*, 82(1977), 371-387.
- [16] J.I. Ramos, Asymptotic analysis of channel flows with slip lengths that depend on the pressure, *Appl. Math. and Computation*, 188(2007), 1310-1318.
- [17] V and V, Viscosity of solutions and suspensions, *Jour. of Phys. and Colloid Chem.*, 52(1948), 277-299.
- [18] T.T. Zhang, L. Jia, Z.C. Wang and X. Li, The application of homotopy analysis method for 2-dimensional steady slip flow in micro channels, *Phys. Lett. A*, 372(2008), 3223-3227.
- [19] T.T. Zhang, L. Jia and Z.C. Wang, Validation of Navier–Stokes equations for slip flow analysis within transition region, *Int J Heat Mass Trans.*, 51(2008), 6323-6327.
- [20] M. Ohki, Unsteady flows in a porous, elastic, circular tube- Part 1: The wall contracting or expanding in an axial direction, *Bulletin of the JSME*, 23(1980), 679-686.
- [21] S.J. Liao, Notes on the homotopy analysis method: Some definitions and theorems, *Comm. Non-Linear Sci. Num. Simul.*, 14(2009), 983-997.
- [22] S.J. Liao, On the relationship between the homotopy analysis method and Euler transform, *Comm. Nonlinear Sci. Numer. Simulat.*, 15(2010), 1421-1431.

- [23] S.J. Liao, On the homotopy analysis method for nonlinear problems, *Appl Math Comput.*, 147(2004), 499-513.
- [24] Y.Z. Boutros, M.B. Abd-el-Malek, N.A. Badran and H.S. Hassan, Lie-group method solution for two-dimensional viscous flow between slowly expanding or contracting walls with weak permeability, *Appl. Math. Modelling*, 31(2007), 1092-1108.
- [25] T. Hayat and M. Khan, Homotopy solution for a generalized second grade fluid past porous plate, *Nonlinear Dyn.*, 42(2005), 395-405.
- [26] N.F.M. Noor and I. Hashim, Thermo capillarity and magnetic field effects in a thin liquid film on an unsteady stretching surface, *Int. J. Heat Mass Trans.*, 53(2010), 2044-2051.
- [27] Kh. S. Mekheimer, M. El-Sabbagh and R.E. Abo-Elkhair, Lie group analysis for the heat transfer in symmetric porous channel with expanding or contracting walls and slip boundary condition, <http://www.etms-eg.org>.